Plasmonic nano-structures for optical data storage

M. Mansuripur,[†] A. R. Zakharian,[‡] A. Lesuffleur,[*] Sang-Hyun Oh,[*] R. J. Jones,[†] N. C. Lindquist,[*] Hyungsoon Im,[*] A. Kobyakov,[‡] and J. V. Moloney[†]

[†]College of Optical Sciences, The University of Arizona, Tucson, Arizona 85721
[‡]Corning Inc., Science and Technology Division, One Science Center Drive, Corning, New York 14831
[*]Department of Electrical and Computer Engineering, University of Minnesota, Minneapolis, MN 55455
masud@optics.arizona.edu

Abstract: We propose a method of optical data storage that exploits the small dimensions of metallic nano-particles and/or nano-structures to achieve high storage densities. The resonant behavior of these particles (both individually and in small clusters) in the presence of ultraviolet, visible, and near-infrared light may be used to retrieve pre-recorded information by far-field spectroscopic optical detection. In plasmonic data storage, a very short (~ few femtoseconds) laser pulse is focused to a diffraction-limited spot over a small region of an optical disk containing metallic nano-structures. The digital data stored in each bit-cell, comprising multiple bits of information, modifies the spectrum of the incident light pulse. This spectrum is subsequently detected, upon reflection/transmission, with the aid of an optical spectrum analyzer. We present theoretical as well as preliminary experimental results that confirm the potential of plasmonic nano-structures for high-density optical data storage applications.

OCIS codes: (210.0210) Optical data storage; (240.6680) Surface plasmons.

References

1. T. W. Ebbesen, H. J. Lezec, H. F. Ghaemi, T. Thio, and P. A. Wolff, "Extraordinary optical transmission through subwavelength hole arrays," Nature **391**(6668), 667–669 (1998).
2. A. G. Brolo, R. Gordon, B. Leathem, and K. L. Kavanagh, "Surface plasmon sensor based on the enhanced light transmission through arrays of nanoholes in gold films," Langmuir **20**(12), 4813–4815 (2004).
3. L. Pang, G. M. Hwang, B. Slutsky, and Y. Fainman, "Spectral sensitivity of two-dimensional nano-hole array surface plasmon polariton resonance sensor," Appl. Phys. Lett. **91**(12), 123112 (2007).
4. A. Lesuffleur, L. K. S. Kumar, and R. Gordon, "Enhanced second harmonic generation from nanoscale double-hole arrays in a gold film," Appl. Phys. Lett. **88**(26), 261104 (2006).
5. A. Lesuffleur, H. Im, N. C. Lindquist, and S.-H. Oh, "Periodic nanohole arrays with shape-enhanced plasmon resonance as real-time biosensors," Appl. Phys. Lett. **90**(24), 243110 (2007).
6. J. J. Mock, S. J. Oldenburg, D. R. Smith, D. A. Schultz, and S. Schultz, "Composite Plasmon Resonant Nanowires," Nano Lett. **2**(5), 465–469 (2002).
7. H. Liu, and P. Lalanne, "Microscopic theory of the extraordinary optical transmission," Nature **452**(7188), 728–731 (2008).
8. A. R. Zakharian, M. Mansuripur, and J. V. Moloney, "Transmission of light through small elliptical apertures," Opt. Express **12**(12), 2631–2648 (2004).
9. Y. Xie, A. R. Zakharian, J. V. Moloney, and M. Mansuripur, "Transmission of light through slit apertures in metallic films," Opt. Express **12**(25), 6106–6121 (2004).
10. N. C. Lindquist, A. Lesuffleur, H. Im, and S.-H. Oh, "Sub-micron resolution surface plasmon resonance imaging enabled by nanohole arrays with surrounding Bragg mirrors for enhanced sensitivity and isolation," Lab Chip **9**(3), 382–387 (2009).
11. M. Mansuripur, *The Physical Principles of Magneto-optical Recording*, Cambridge University Press, Cambridge, United Kingdom, 1995.
12. J. F. Heanue, M. C. Bashaw, and L. Hesselink, "Volume holographic storage and retrieval of digital data," Science **265**(5173), 749–752 (1994).
13. W. E. Moerner, *Persistent Spectral Hole-Burning: Science and Applications*, Springer (1988).
14. J. Strickler, and W. Webb, "Three-dimensional optical data storage in refractive media by two-photon point excitation," Opt. Lett. **16**(22), 1780–1782 (1991).
15. S. Kawata, and Y. Kawata, "Three-dimensional optical data storage using photochromic materials," Chem. Rev. **100**(5), 1777–1788 (2000).

#112667 - $15.00 USD Received 11 Jun 2009; revised 14 Jul 2009; accepted 15 Jul 2009; published 28 Jul 2009

16. D. Day, M. Gu, and A. Smallridge, "Rewritable 3D bit optical data storage in a PMMA-based photorefractive polymer," Adv. Mater. **13**(12-13), 1005–1007 (2001).
17. P. Zijlstra, J. W. M. Chon, and M. Gu, "Effect of heat accumulation on the dynamic range of a gold nanorod doped polymer nanocomposite for optical laser writing and patterning," Opt. Express **15**(19), 12151–12160 (2007).
18. P. Zijlstra, J. W. M. Chon, and M. Gu, "Five-dimensional optical recording mediated by surface plasmons in gold nano-rods," Nature 08053 (2009).
19. M.Mansuripur, A.R.Zakharian, A.Kobyakov and J.V.Moloney, "Plasmonic nano-structures for optical data storage," Paper WA2, Abstracts Booklet, *ISOM/ODS'08*, Hawaii, July 2008.
20. M. Mansuripur, A. R. Zakharian, Sang-Hyun Oh, R. J. Jones, A. Lesuffleur, N. C. Lindquist, Hyungsoon Im, A. Kobyakov, and J. V. Moloney, "Plasmonic Optical Data Storage," Paper TuA3, Abstracts Booklet, *ODS'09*, Orlando, Florida, May 2009.
21. J. Chou, D. R. Solli, and B. Jalali, "Real-time spectroscopy with subgigahertz resolution using amplified dispersive Fourier transformation," Appl. Phys. Lett. **92**(11), 111102 (2008).

1. Introduction

Metallic nano-structures exhibit strong resonances when illuminated with ultraviolet, visible, or near-infrared light in the vicinity of their surface plasmon polariton (SPP) frequencies [1-10]. These SPP resonance frequencies are sensitive to the geometry and dimensions of the nano-structure, e.g., diameter and depth of a pit or a hole in a metal film, diameter and length of a metallic nano-rod, axial dimensions of an ellipsoidal nano-particle, etc. The resonances are also dependent on the orientation of the nano-structure relative to the polarization state of the incident light [7,8]. In addition to sensitivity to polarization and wavelength, metallic nano-structures exhibit strong interactions with their environment and with each other; for example, optical transmission through one nano-hole is strongly modulated by the presence of other nano-holes in the neighborhood [10].

In this paper we describe a method of optical data storage that exploits the small dimensions of metallic nano-structures and nano-particles to achieve high storage densities and high data rates. The proposed method employs the resonant behavior of nano-structures and/or nano-particles (both individually and in small clusters) for the purpose of retrieving the stored information using spectroscopic far-field detection. The nano-features should be arranged in such a way as to imprint their signature in a unique way on the optical spectrum of the readout laser beam. It should be emphasized at the outset that the large-scale fabrication of such nano-structures in a reliable and cost-effective way is far from trivial for the present-day manufacturing technologies. It is our hope, however, that an exploration of plasmonic nano-structures in the context of optical data storage will bring attention to the unique properties and potential advantages of such structures, thus spurring the development of tools and techniques for their large-scale fabrication.

Conventional methods of optical disk data storage as employed in Compact Disc (CD), Digital Versatile Disc (DVD), and Blue Ray Disc (BD), as well as in the recordable and rewritable versions of these media are well-known [11]. Holographic optical storage has been under research and development for nearly half a century [12] and, in recent years, a commercial holographic data storage system has been introduced into the market by *InPhase Technologies* of Longmont, Colorado. Many alternative methods of optical data storage have been proposed over the years, based either on new material systems or on novel read/write/erase schemes. We mention spectral hole-burning [13], three-dimensional (3D) optical storage by two-photon point excitation [14], 3D storage in photochromic and photorefractive materials [15,16], and the recently announced five-dimensional optical recording mediated by surface plasmons in gold nano-rods [17,18]. The plasmonic scheme of optical data storage presented in the following sections has some similarities but also major differences with the plasmon-mediated method employed by Zijlstra *et al* [18]. We compare the two methods in the final section of this paper and point out their similarities and differences. In the intervening sections we introduce the principle of plasmonic data storage and demonstrate the feasibility of the concept using numerical simulations and experimental data obtained from nano-apertures milled in thin silver films.

#112667 - $15.00 USD Received 11 Jun 2009; revised 14 Jul 2009; accepted 15 Jul 2009; published 28 Jul 2009

2. Basic concept of plasmonic data storage

We introduced the general principles of plasmonic optical storage at the joint meeting of the *International Symposium on Optical Memory* (*ISOM*) and the *Optical Data Storage Conference* (*ODSC*) in July 2008 [19], followed by a more detailed presentation at the *ODSC* in May 2009 [20]. In the proposed scheme, a very short laser pulse (duration ~ a few femto-seconds, i.e., a super continuum source) is focused to a diffraction-limited spot on a sub-micron-sized area of an optical disk, which contains plasmonic nano-structures. Each such plasmonic structure, referred to as a bit-cell, is a collection of nano-scale holes and/or slits within a thin metallic film. (Alternatively, a cluster of metallic nano-particles or nano-rods embedded in a transparent substrate may constitute the plasmonic nano-structure associated with each bit-cell.) Each bit-cell contains several (e.g., a dozen or more) bits of user-data within its embedded nano-structure. Dimensions of the bit-cell are defined by the volume of material that is illuminated by the focused laser beam, namely, (area of focused spot) × (depth of focus). The information stored in each bit-cell modifies the spectrum of the incident super continuum light pulse, which is subsequently detected in transmission (or reflection) with the aid of an optical spectrum-analyzer.

Figure 1 shows a possible realization of an optical storage medium that incorporates nano-holes and/or nano-slits in a thin metallic film. The data bits are grouped together in small clusters and placed within individual bit-cells, each cell containing several bits of information. As an example, a typical bit-cell may occupy a $0.5 \times 0.5\,\mu m^2$ area on the surface of a 0.2 μm-thick silver film, each bit-cell containing ten or more nano-holes whose individual diameters could range from, say, 20 to 100 nm. If, in a given cluster, the presence or absence of a nano-hole of a specific-size is associated with a single information bit ("0" or "1"), then m nano-holes can encode an m-bit sequence within each bit-cell. Transmission of light through a nano-hole (or nano-slit) is a strong function of the aperture diameter and film thickness, as well as the size, shape, and location of the neighboring nano-apertures. For a given state of polarization of the incident beam, certain wavelengths couple strongly to the guided mode through a nano-aperture and reach the opposite side, while other wavelengths are either reflected from the metallic surface or resonantly transmitted through adjacent nano-apertures; see Fig. 2. It is this property of nano-holes and nano-slits that provides a mechanism for readout of the stored information. (Although Fig. 1 shows one track containing nano-holes and an adjacent track containing nano-slits, there is no a priori reason for distinguishing between the two; in other words, it should be possible to mix nano-slits with circular as well as elliptical nano-holes in arbitrary combinations and arrangements.)

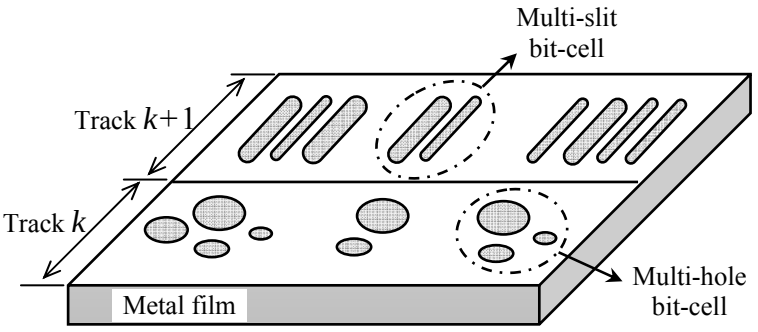

Fig. 1. In one realization of the proposed concept, plasmonic features are nano-holes and/or nano-slits in a thin metallic film. A group of such features constitutes a bit-cell, within which several bits of information are encoded in a small (micron-sized) region of the storage medium. Much like the organization of data on a conventional optical disk, these bit-cells are arranged sequentially along parallel data tracks.

#112667 - $15.00 USD Received 11 Jun 2009; revised 14 Jul 2009; accepted 15 Jul 2009; published 28 Jul 2009

3. Numerical simulations

Computer simulations indicate that the transmission spectra of nano-hole and/or nano-slit clusters in thin metallic films exhibit multiple resonance peaks, which can be used to identify the structure during readout. Figure 2(a) shows a number of transmission spectra computed with the FDTD method for a 250 nm-thick silver film suspended in free space. Single, double, and triple nano-holes with various spacings, all filled with a dielectric of refractive index n_o=2.0, are depicted in this figure. The assumed wavelengths cover the visible range of 400−700 nm, although, in principle, the range can be extended to the ultraviolet and near-infrared wavelengths as well. Similar transmission curves for multiple air-filled (i.e., n_o=1.0) nano-slits in a suspended 400 nm-thick silver film are shown in Fig. 2(b).

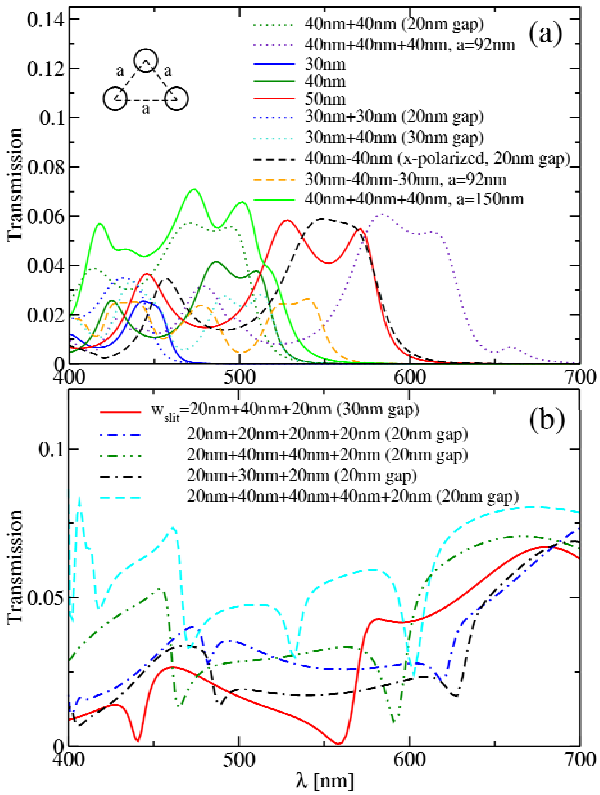

Fig. 2. Computed transmissivity versus the vacuum wavelength λ for (a) nano-holes and (b) nano-slits in a silver slab. The Finite Difference Time Domain (FDTD) method has been used to solve Maxwell's equations; transmissivity is defined as the fraction of total incident optical power at each wavelength. The regions on both the incidence and transmission sides of the silver slab are free-space (n = 1), and the Drude model is used to simulate the dispersion of the complex dielectric constant $\varepsilon(\omega)$ of silver.

(a) The 250 nm-thick silver film contains single, double, and triple cylindrical holes of varying diameters, as indicated in the legend by the radii of the holes. All the holes are filled with a transparent dielectric of refractive index n_o = 2.0. The incident beam is a focused Gaussian, linearly-polarized along the y-axis, and having FWHM = 1 μm. The waist of the focused spot is in the xy-plane at a distance of Δz = 55 nm above the top surface of the silver film. Variations of transmissivity with λ are due to resonances within each hole as well as plasmonic coupling between adjacent holes.

(b) Multiple air-filled slits (n_o = 1) having widths W_1 = 20 nm, W_2 = 30 nm, and W_3 = 40 nm. Different combinations of these slits are embedded within a 400 nm-thick silver film and illuminated with a focused Gaussian beam. Each cluster of slits has a unique transmission spectrum, which could be exploited for identification of the cluster during readout.

#112667 - $15.00 USD Received 11 Jun 2009; revised 14 Jul 2009; accepted 15 Jul 2009; published 28 Jul 2009

Optical properties of the substrate and the surrounding layers, if any, play an important role in determining the details of the transmission/reflection spectra. For example, Fig. 3(a) shows the transmission spectra of a 100 nm-diameter hole (filled with n_o=2.0 dielectric) with and without a substrate. Presence of a substrate (n_{sub}=1.5) changes the transmissivity of the nano-hole from the red curve to the blue curve. Furthermore, removing the dielectric filling shifts the transmission peak to UV wavelengths, with the result that no visible light is transmitted through an empty 124 nm-diameter hole in a 200 nm-thick silver film coated on a glass substrate (green curve).

In Fig. 3(b) the profile of E_z, the E-field component of the focused light perpendicular to the silver film's surface, indicates the excitation of surface plasmon polaritons (SPPs) in the vicinity of a pair of 100 nm-diameter holes separated in the y-direction by 150 nm. Such resonance phenomena, of course, are partly responsible for the peaks and valleys of the transmission spectra of plasmonic nano-structures, with the other relevant factor being the Fabry-Perot-like resonance inside the holes. More detailed results of these numerical simulations are given in the Appendix.

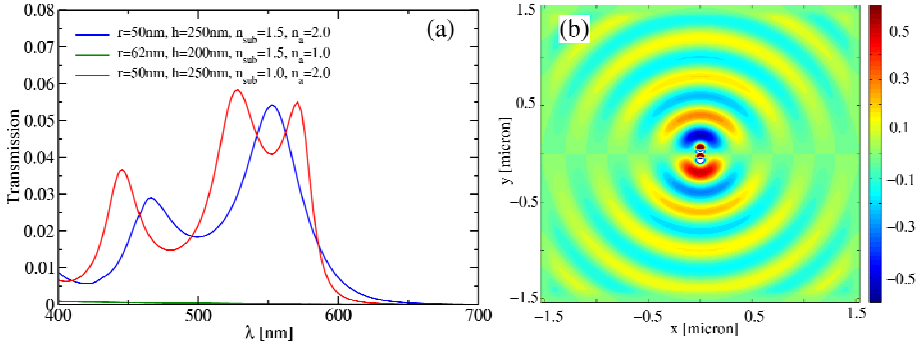

Fig. 3. (a) The red curve is the transmission spectrum of a single, 100 nm-diameter hole filled with n_o=2.0 dielectric in a 250 nm-thick, free-standing silver slab; this is the same curve as that shown in Fig.2(a) – also in red. The blue curve is similar, except for the silver film being deposited on an n_{sub}=1.5 glass substrate (the hole continues to be filled with n_o=2.0 dielectric). The green curve at the bottom of the frame corresponds to a 124 nm-diameter hole in a 200 nm silver film deposited atop an n_{sub}=1.5 substrate. (b) Plot of instantaneous E_z in the xy-plane at Δz = 5nm below the bottom facet of a silver film containing a pair of nano-holes. The plot reveals the excitation of SPP on both sides of the nano-hole pair along the direction y of incident polarization.

4. Readout scheme

A readout method for the nano-apertures of Fig. 1 is shown in Fig. 4. Here a short pulse from a femtosecond laser, compressed further by a photonic crystal fiber or otherwise to produce a super continuum source, is focused on a bit-cell, and the transmitted beam is subsequently sent to a spectrum analyzer. The pulse is short enough (~ few fs) that its spectrum covers the entire range of visible frequencies. Each cluster of nano-apertures is thus uniquely identified by its spectral signature, and the entire content of the bit-cell is retrieved upon analyzing the spectrum of the transmitted light. Assuming a linear track-velocity of 100 m/s and a focused spot-size of ~0.5 μm, the dwell time on each bit-cell is ~5 ns, thus requiring a repetition rate of ~200 MHz from the super continuum light source. If one further assumes that a maximum of 10 bits – exhibiting 2^{10}=1024 distinct transmission spectra – can be stored within a bit-cell, the resulting data-rate will be ~2 Gbit/s.

Assuming the laser beam delivers an average optical power of 1–2 mW to the disk, the integrated power of the focused spot over the xy-plane of the disk (and over the useful spectral bandwidth of the light pulse) will be around 1–2 mJ/s. With a pulse repetition rate of ~200 MHz and a linear track velocity of ~100 m/s, the focused spot moves a distance of

#112667 - $15.00 USD Received 11 Jun 2009; revised 14 Jul 2009; accepted 15 Jul 2009; published 28 Jul 2009

0.5 μm on the disk surface in the time interval between adjacent pulses; this is roughly the diameter of the diffraction-limited spot. The number of photons in each such pulse is $\sim 10^7$, which, even with 1% transmission efficiency through the disk, will result in $\sim 10^5$ photons (per pulse) arriving at the detector. If we suppose that a 100-element array of photodetectors is needed to monitor the transmitted spectrum, each individual detector will receive $\sim 10^3$ photons per pulse, which should be readily detectable with the current silicon photodiode technology. (More efficient and less cumbersome methods of spectral monitoring are also available. For example, the transmitted pulse can be sent through a short length of dispersive optical fiber, which Fourier transforms its spectrum into the time domain [21]. A single fast photodetector can then read the entire spectral content of the pulse as a function of time.)

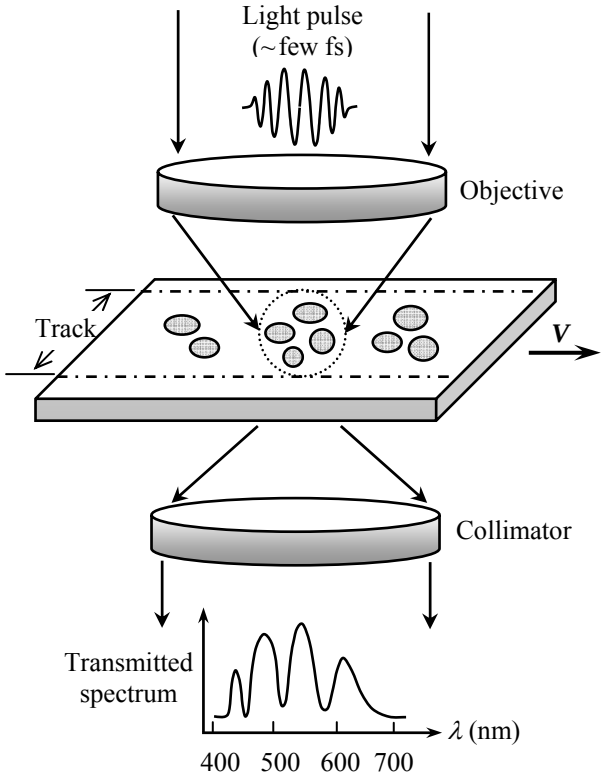

Fig. 4. Proposed readout scheme for the plasmonic disk depicted in Fig. 1. A very short laser pulse (duration ~ few femtoseconds) is focused by a diffraction-limited objective onto the disk surface. The pulse has a broad spectrum, covering the entire visible range ($\lambda = 400$ nm to 700 nm) and possibly beyond. The size of the focused spot at the disk surface, ~0.5μm, is comparable to the bit-cell dimensions. Although the nano-holes within a given cell are *not* individually resolved in a conventional sense, their collective signature, imprinted upon the spectrum of the transmitted light, can be used to identify the presence or absence of various holes within a cell. With a maximum of 10 nano-holes placed in each cell, for example, the total number of distinct spectral patterns will be $2^{10} = 1024$. The spectral patterns can be further optimized by adjusting the nano-holes' shape/size/position relative to each other and also relative to the direction of polarization of the incident beam.

The energy content of an incident light pulse, given the aforementioned set of parameters, is $\sim 5-10$ pJ. Assuming 25–50% energy absorption in the metallic film (or other metallic nano-structure), given that a material volume of $\sim 10^{-13}$ cm^3 is typically heated by each pulse, the temperature rise should not exceed 10–20°C (silver's heat capacity, for instance, is ~2.4 J/cm^3/°C). Therefore, as far as material integrity and longevity are concerned, this level of heating should not pose any serious problems.

#112667 - $15.00 USD Received 11 Jun 2009; revised 14 Jul 2009; accepted 15 Jul 2009; published 28 Jul 2009

We emphasize that pulsed laser operation is crucial for this application. The plasmonic patterns recorded on the disk respond differently to different positions of the focused spot relative to the bit-cell. In the proposed readout scheme, the bit-cell is essentially stationary during the short period of the light pulse. Assuming that the pulse is synchronized with the bit-cell centers along the track, the spectrum of each transmitted pulse will be a pre-determined function of frequency, which can be readily associated with the plasmonic structure recorded in the bit-cell. If, instead, a cw light source is used for readout, the spectral signature of the bit-cell will change with time as the disk rotates, producing intersymbol interference between adjacent bit-cells, and making the recognition of the spectral signature (and association with a unique plasmonic structure) much more difficult. Also crucial for our application is the spatial coherence of the light source, as the incident beam needs to be focused into a diffraction-limited spot with a significant concentration of optical energy, a task that cannot be achieved with an incoherent light source such as a light emitting diode.

5. Experimental results

Figure 5 shows the structure of the samples we have fabricated in a silver film in order to verify the predicted optical behavior of nano-holes in a metallic host. A 300 nm Si_3N_4 layer was initially grown over the Si substrate. The Si substrate was subsequently etched away through anisotropic etching to create a $200\times200\,\mu m^2$ suspended nitride membrane. This was followed by a 200 nm-thick silver film deposition atop the nitride layer. Using the focused ion-beam (FIB) technique, a $10\times10\,\mu m^2$ square of Si_3N_4 was removed to create a free-standing silver layer through which nano-holes with a wide range of diameters and separations were milled. Figure 5(b) shows FIB images of single, double, and triple nano-holes (diameter d=100 nm) within the 200 nm-thick silver film. The geometric parameters of the circular and elliptical hole pairs are defined in Figs. 5(c) and 5(d), respectively.

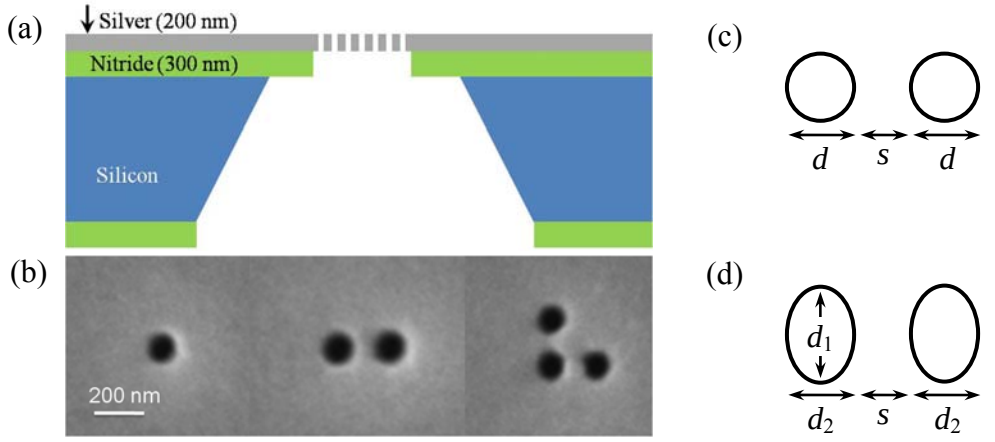

Fig. 5. (a) Cross-sectional diagram and (b) FIB images showing nano-holes drilled into a free-standing 200 nm-thick silver film on a 300 nm-thick silicon nitride membrane. The silicon substrate and the nitride layer are etched away from the region directly beneath the nano-holes. The FIB images show single, double, and triple nano-holes, each having a diameter of ~100 nm. (c) Circular hole-pairs have diameter d and edge-to-edge separation s. (d) Elliptical hole-pairs have diameters (d_1, d_2) and edge-to-edge separation s.

The measured transmission spectra of single, double, and triple nano-holes for the sample depicted in Fig. 5 are shown in Fig. 6. These measurements were carried out with an unpolarized white-light source and a conventional spectro-photometer. The measured structures differ from those simulated in Fig. 2(a) in that the nano-holes were not filled with a high-index dielectric material. Nevertheless, the general behavior of transmission spectra in

#112667 - $15.00 USD Received 11 Jun 2009; revised 14 Jul 2009; accepted 15 Jul 2009; published 28 Jul 2009

Fig. 6 agrees qualitatively with that expected from the simulations. In particular, the differences between the spectra of different hole-patterns are large enough to enable reliable readout of the various structures. Similar results for single and double nano-holes in a different sample are shown in Fig. 7, where a 2 μm−diameter aperture was milled in the silver film to improve the calibration procedure.

A quantitative comparison of the measured transmission spectra with FDTD simulation results proved difficult, presumably because the dielectric function $\varepsilon(\omega)$ of bulk silver does not properly represent the optical properties of thin silver films used in our experiments.

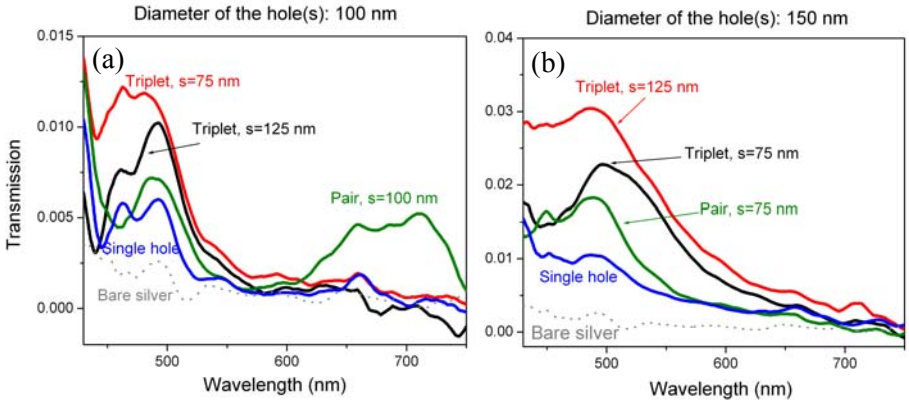

Fig. 6. Measured transmission spectra through single, double, and triple circular nano-holes in the suspended 200 nm silver film depicted in Fig. 5. The white-light source used in these measurements was unpolarized, the holes were air-filled, and an incident optical power density of unity/μm^2 was assumed. In the absence of nano-holes, the film's transmissivity is below 0.3% (dotted gray curve). Hole diameters are 100 nm in (a) and 150 nm in (b).

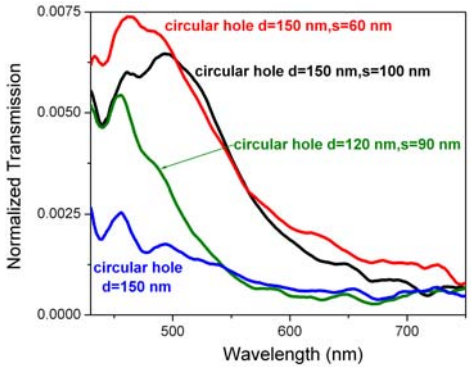

Fig. 7. Measured transmission spectra through single and double circular apertures in the suspended 200 nm silver film depicted in Fig. 5. The white-light source was unpolarized. The spectra are normalized by the transmissivity of a 2 μm−diameter aperture milled in the silver film. Blue: single hole, d=150 nm. Green: hole pair, d=120 nm, s=90 nm. Red: hole pair, d=150 nm, s=60 nm. Black: hole pair, d=150 nm, s=100 nm.

From these and similar measurements we learn that a single 100 nm-diameter hole (blue curve in Fig. 6(a)) has approximately 0.5% transmission below $\lambda \sim 500$ nm. Double-holes of the same diameter, having separations of 75, 100 and 125 nm, have nearly identical transmission spectra, with a peak transmissivity of ~0.75% around $\lambda \sim 500$ nm. The triplets, having separations of 75, 100 and 125 nm, show as much as 0.9−1.2% transmissivity within the $\lambda \sim 450-500$ nm band. For the 150 nm holes depicted in Fig. 6(b), compared to 100 nm holes depicted in Fig. 6(a), the transmission level is higher across the board, the peak

#112667 - $15.00 USD Received 11 Jun 2009; revised 14 Jul 2009; accepted 15 Jul 2009; published 28 Jul 2009

transmission has shifted to slightly longer wavelengths, and transmissivity at longer wavelengths (i.e., $\lambda \sim 550-650\,\text{nm}$) is substantially higher. Transmission through triple holes is generally greater than that through double holes, which is in turn greater than that through a single hole. Double-hole transmissivity appears to be insensitive to hole separation, whereas the separation distance for triple holes makes a substantial difference in the short-wavelength end of the spectrum (i.e., $\lambda \sim 425-500\,\text{nm}$).

Figure 8 shows the measured transmission spectra for single and double elliptical holes in the suspended, 200 nm-thick silver film depicted in Fig. 5. The white-light source used in these measurements was linearly polarized parallel to the short axis of the apertures in the case of Fig. 8(a), and perpendicular to that axis in the case of Fig. 8(b). The transmitted optical power was calibrated with the aid of a 2 μm-diameter hole milled in the silver film. Once again, the spectra are seen to be sufficiently different to provide unique signatures not only for each nano-structure, but also for different orientations of these structures relative to the direction of incident polarization. When the incident polarization is parallel to the short axis, transmission could be as high as 1.5% for the larger pair of ellipses at and around $\lambda = 600\,\text{nm}$. In general, these elliptical hole-pairs show four to five times greater transmission in the green-red range of wavelengths compared to a single aperture. When the incident polarization is parallel to the long axis of the ellipse, transmission peaks shift to the blue end of the spectrum ($\lambda \sim 400\text{-}500\,\text{nm}$), and the maximum transmission drops to the range between 0.3 - 0.6%, depending on aperture size and separation between the apertures.

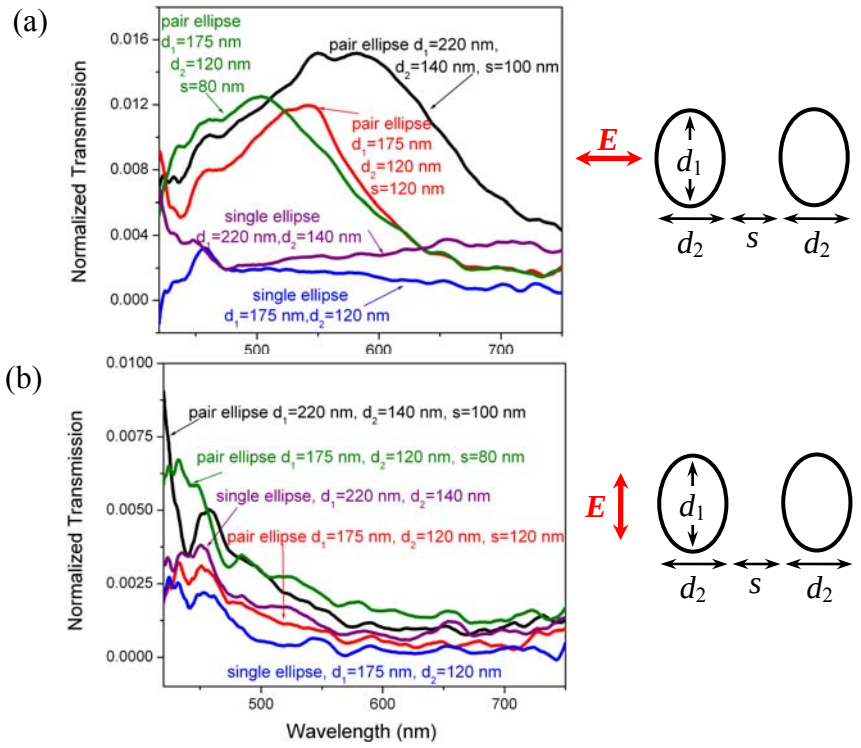

Fig. 8. Measured transmission spectra through single and double elliptical nano-holes in the suspended 200 nm-thick silver film depicted in Fig. 5. The white-light source used in these measurements was linearly polarized (a) parallel to the short axis, (b) parallel to the long axis of the elliptical apertures. The spectra, labeled by aperture diameters (d_1, d_2) and pair separation s, are normalized by the transmissivity of a 2 μm-diameter aperture milled in the silver film.

#112667 - $15.00 USD Received 11 Jun 2009; revised 14 Jul 2009; accepted 15 Jul 2009; published 28 Jul 2009

All in all, spectral features in the case of polarization parallel to the long axis are less pronounced compared to those obtained when polarization is parallel to the short axis. Extending the observation wavelengths to violet and UV (say, $\lambda \sim 300-400\,\text{nm}$) may be necessary in order to take full advantage of elongated apertures whose long axes are to be aligned (or nearly aligned) with the direction of incident polarization. Alternatively, one may use high-index dielectric fillers to shift the resonance wavelengths toward the red end of the spectrum. In general, a combination of both techniques might be necessary if there is a desire to incorporate very small apertures (e.g., $d < 100\,\text{nm}$) within the bit-cells.

We also measured the transmission spectra of some of the circular as well as elliptical hole-pairs using a super continuum light source (i.e., femto-second pulsed laser followed by a photonic crystal fiber); the results are shown in Fig. 9(a). The polarization state of this light source was not determined; therefore, the measured spectra represent a mix of the two linear polarization states used previously in conjunction with the white-light source. Nevertheless, the qualitative features of the spectra obtained with our super continuum source are in good agreement with those obtained with the white-light source. The presence of the 2 μm-diameter calibration aperture on the sample was crucial for the proper normalization of these spectra. Once again, the pair of large elliptical apertures showed high transmissivity, i.e., 1.0 – 1.2%, in the range of $\lambda \sim 500-650\,\text{nm}$. The smaller apertures exhibited lower transmissivity, and their spectra were concentrated in the blue-green part of the visible spectrum.

Finally, we used our super continuum light source to obtain the transmission spectra of some samples that were fabricated on a glass substrate. In this case we covered the nano-holes (milled in the silver film) with a droplet of index-matching fluid ($n_o \sim 1.5$). The results are shown in Fig. 9(b). In these experiments the light pulses were not sufficiently stable, and the results are not quite as reliable as those of Fig. 9(a). Nevertheless, one can see substantial differences between the spectra of different hole-patterns. Such differences, when monitored with stable femto-second pulses, are expected to provide sufficient information to enable reliable readout of the recorded information in a plasmonic data storage system.

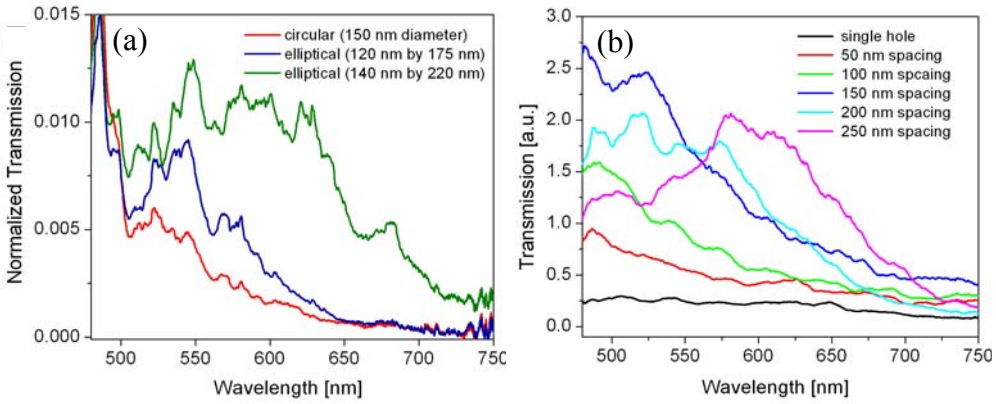

Fig. 9. Transmission spectra through nano-apertures measured with a *super continuum* source. (a) Pairs of air-filled circular and elliptical apertures in a suspended 200 nm-thick silver film. The circular holes (red) have $d = 150\,\text{nm}$. In the case of elliptical holes, major and minor diameters (d_1, d_2) are ($175\,\text{nm} \times 120\,\text{nm}$) (blue) and ($220\,\text{nm} \times 140\,\text{nm}$) (green). Separation between the apertures is $s = 100\,\text{nm}$ in all cases. (b) Single and double circular holes having diameter $d = 100\,\text{nm}$. The 200 nm-thick silver film is deposited on a glass substrate. A droplet of index-matching fluid ($n_o \sim 1.5$) is placed atop the silver surface prior to measurements. Vertical scale is not normalized. While transmission through the single hole (black curve) is relatively weak, double holes exhibit progressively stronger transmission with increasing hole separation. The spectra of double-holes with separation $\geq 150\,\text{nm}$ extend as far as $\lambda \sim 700\,\text{nm}$. In both (a) and (b), the various spectra are clearly distinguishable from each other, each representing a unique signature for the corresponding hole pattern.

#112667 - $15.00 USD Received 11 Jun 2009; revised 14 Jul 2009; accepted 15 Jul 2009; published 28 Jul 2009

6. Alternative design: embedded nano-rods and stacked multilayer disk

Unless the number of stored bits in individual cells can reach 10 and beyond, it is difficult for the proposed device of Fig. 1 to surpass the storage capacity of a conventional Blu-Ray disk, i.e., 25GB per layer on a 12 cm platter. A variation on the same theme, however, is shown in Fig. 10, where information is stored in metallic nano-rods embedded in a transparent substrate. Each nano-rod resonates with one or more wavelengths within the UV−visible−near-IR range, scattering the resonant wavelength(s) out of the main optical path [6]. The transmitted light's spectrum is thus endowed with the collective signature of the cluster of rods embedded within individual bit-cells. This alternative scheme for plasmonic data storage has the advantage that a large fraction of the incident light can pass through each storage layer, thus allowing the stacking of several such layers. The cross-talk among these layers may be negligible so long as the separation between adjacent layers is large enough for the focused cone of laser light to average over a large number of bit-cells in each of the adjacent layers.

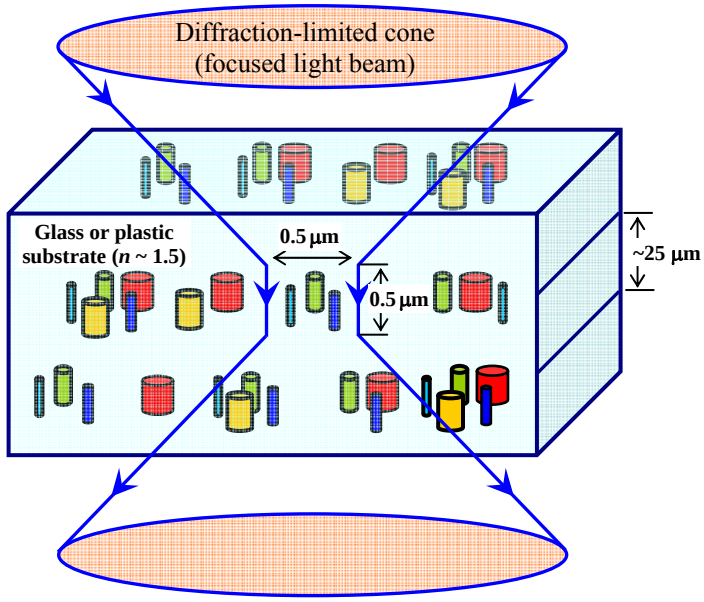

Fig. 10. An alternative realization of the concept of plasmonic data storage. Each bit-cell is a collection of metallic nano-rods (diameter ~ 20−100 nm, height ~ 1.0 μm) embedded in a transparent substrate. Identical rods appear in different cells, although a given cell may or may not contain a specific-sized rod. Each cell stores *m* information bits in the form of the presence or absence of a given rod (0 or 1). The incident beam is a diffraction-limited cone of light with a spot diameter of ~ 0.5μm and a duration of a few femtoseconds. Since nano-rods of differing dimensions resonate at different wavelengths, the scattering cross-section of each rod is a strong function of the incident wavelength. Provided that attenuation is not too severe, the light pulse may pass through several layers of nano-rods before focusing on a specific cell. The transmitted spectrum thus carries the signature of the bit-cell located within the focal volume.

Results of FDTD computer simulations for a 500 nm-long, 80 nm-diameter silver nano-rod embedded in a transparent substrate of refractive index $n=1.5$ are shown in Fig. 11. The incident beam is a focused Gaussian of FWHM = 1μm, $\lambda=458$ nm, located at $\Delta z=55$ nm above the upper surface of the nano-rod and linearly polarized along the *y*-axis. The incident wavelength is chosen to produce SPP resonance along the length of the nano-rod, thereby producing maximum scattering.

In Figure 12 we show computed transmission spectra of single, double, and triple nano-rods, all having a length of 500 nm and embedded in a transparent substrate of refractive index $n=1.5$. For the smallest rod ($d=60$ nm), the nano-rod is almost invisible at longer

#112667 - $15.00 USD Received 11 Jun 2009; revised 14 Jul 2009; accepted 15 Jul 2009; published 28 Jul 2009

wavelengths, but transmission drops to about 90% below $\lambda = 500\,\text{nm}$. As the diameter of the rod increases, the transmissivity minimum shifts to longer wavelengths. For double and triple nano-rods, the transmissivity minima are further shifted to longer wavelengths and the pattern of resonances can be used to uniquely identify the nano-structure.

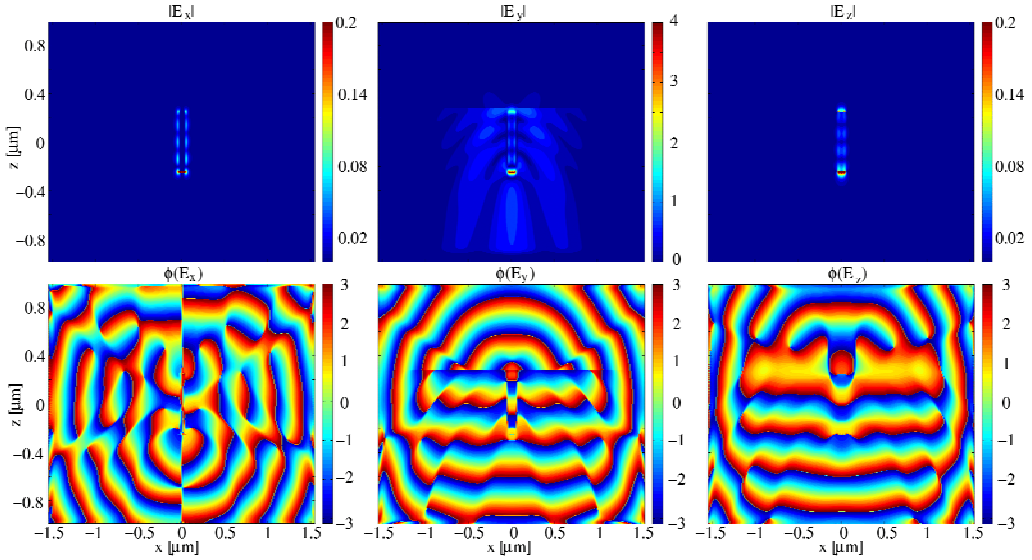

Fig. 11. Plots of amplitude and phase in the *xz* cross-sectional plane for a 500 nm-long silver nano-rod (cylinder radius $r = 40\,\text{nm}$) at the resonance wavelength of $\lambda = 458\text{nm}$. The incident beam is a focused Gaussian having FWHM = 1 μm, located at $\Delta z = 55\,\text{nm}$ above the upper surface of the nano-rod and linearly polarized along the *y*-axis. From left to right: E_x, E_y, E_z components of the electric field. Top row: amplitude; bottom row: phase.

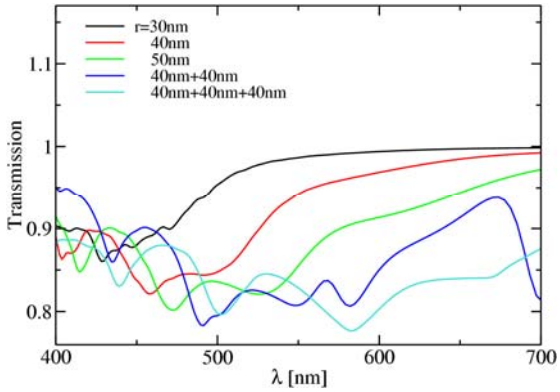

Fig. 12. Computed transmission spectra of 500 nm-long cylindrical nano-rods of differing diameters ($d = 60, 80, 100\,\text{nm}$), embedded in a dielectric host of refractive index $n = 1.5$. The incident focused spot has FWHM = 1.0 μm and is linearly polarized along the *y*-axis. The spectra of individual nano-rods are plotted in black, red and green. The dark-blue curve corresponds to a pair of 80 nm-diameter nano-rods, while the light-blue curve represents the transmission spectrum of three 80 nm-diameter rods placed at the vertices of a triangle.

7. Concluding remarks

We have proposed the concept of plasmonic data storage, which exploits optical resonances that occur on the surfaces of metallic films, inside nano-holes and nano-slits milled into such films, and over the length of metallic nano-rods embedded in transparent substrates. Information is encoded into such metallic nano-structures that are placed either on the surface of an optical disk or throughout the entire volume of a 3D storage medium. Based on the

#112667 - $15.00 USD Received 11 Jun 2009; revised 14 Jul 2009; accepted 15 Jul 2009; published 28 Jul 2009

results of computer simulations and also experimental data from nano-apertures in thin silver films presented in this paper, we believe the concept is feasible. It remains to be seen whether such structures can be fabricated on a large scale, and whether the readout of information can be accomplished at high enough speed and reliability to make the concept worthy of commercialization.

The plasmonic scheme of optical data storage presented in this paper has similarities but also major differences with the plasmon-mediated method employed by Zijlstra *et al* [18]. For example, our method provides for read-only storage of information involving pre-patterned nano-apertures in metallic films, as well as nano-rods or nano-particles of arbitrary shapes embedded in a pre-patterned transparent host. In contrast, the method of Zijlstra *et al* is a write-once-read-many storage technique based on metallic nano-rods of differing aspect-ratios all mixed together and applied uniformly over the entire surface of an optical disk. In our method, the use of very short light pulses (~a few femtoseconds) is essential, as we rely on a broad optical spectrum that covers the entire visible range of wavelengths (and beyond) to simultaneously extract all the information stored within a given bit-cell. In contrast, Zijlstra *et al* use much longer laser pulses (~100 fs) and, do not require a broad spectrum at all. In fact, they even mention that the use of femtosecond pulses in their experiments is incidental, and that the same results could be obtained by much longer (e.g., nanosecond) pulses, so long as each pulse carries enough energy to produce a photo-thermal deformation of the resonant nano-rods [18]. Zijlstra *et al* need the spectrum of their light pulses to be sufficiently narrow to select specific groups of resonant nano-rods, whereas our laser pulses must have a very broad spectrum to excite all the resonances at once.

The method of readout proposed by Zijlstra *et al* is based on two-photon luminescence, whereas we employ the (linear) plasmonic resonances for readout. Zijlstra *et al* use polarization of the light beam to select different orientations of rods having similar aspect ratios within their storage medium, whereas in our scheme the light pulse will always have the same polarization state; we take advantage of the polarization dependence of the resonances by incorporating nano-structures into pre-patterned media that produce different transmission spectra upon illumination by the same light pulse.

All in all, we believe that the two plasmon-based methods, rather than being in competition with each other, are complementary, in the sense that one could perhaps use "individually programmed" super continuum light pulses to write multiple bits simultaneously in the plasmonic media proposed by Zijlstra *et al*. Similarly, our method of readout could be combined with their method of recording to extract multi-bit information from the same region of the storage medium under a focused laser beam.

Appendix

We present results of FDTD simulations for transmission of a focused beam of light through triple nano-holes located at the vertices of an equilateral triangle in a suspended silver film. Figure A1 shows profiles of the *E*-field amplitude (top) and phase (bottom) for a triplet of $r = 4$ nm holes filled with $n_o = 2.0$ dielectric in a 250 nm-thick silver film at $\lambda = 473$ nm (peak of transmission); the film is suspended in free space ($n = 1$). The holes are at the vertices of an equilateral triangle (side = 150 nm) centered at the origin, with one hole centered on the *y*-axis. The source plane of the incident Gaussian beam, linearly-polarized along the *y*-axis and having FWHM = 1 μm, is at $\Delta z = 55$ nm above the top surface of the film.

Figure A1 shows, from left to right, the *x*, *y*, *z* components of the *E*-field at $\Delta z = 5$ nm below the bottom facet of the silver film. The E_z plot shows the location of the electric charge accumulated near the edges of the holes. Figure A2 shows the field profiles through a cross-section of the silver film; the cross-section is at the *yz*-plane, with the cut going through the center of one hole and in between the other two holes. One can clearly see in the $|E_y|$ plot the penetration of the incident radiation through the skin depth of the silver film. The *E*-field inside the hole is strongly resonant, as seen by the strong $|E_y|$ component of the field within

#112667 - $15.00 USD Received 11 Jun 2009; revised 14 Jul 2009; accepted 15 Jul 2009; published 28 Jul 2009

the hole, and also by the accumulated charges near the edges of the hole at the top and bottom of the silver film. As can be seen from the light-green curve in Fig. 2(a), the transmissivity of the triple hole under the conditions shown in Figs. A1 and A2 (i.e., at $\lambda = 473$ nm) is ~7%.

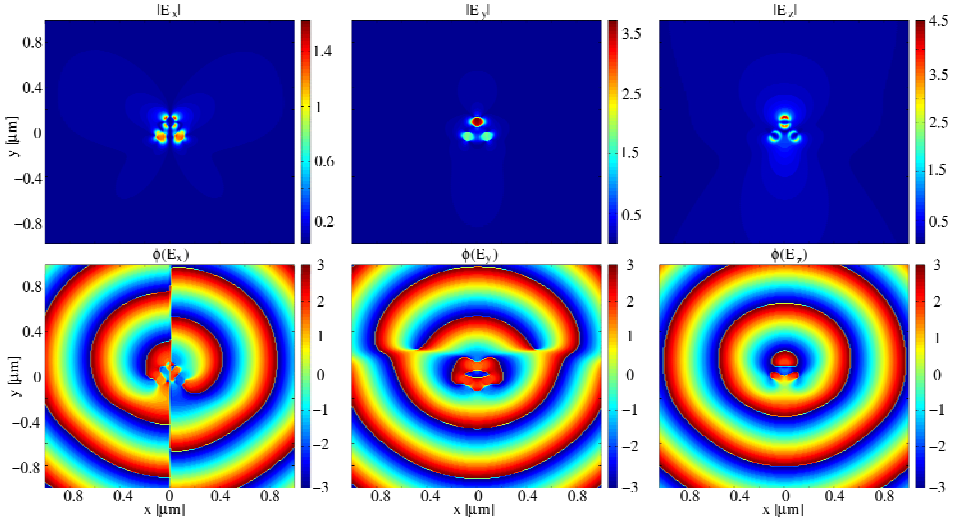

Fig. A1. Amplitude and phase plots on the bottom facet of a 250 nm-thick silver film when a focused beam goes through a triplet of 80 nm-diameter holes. The holes are filled with $n_o = 2.0$ dielectric, their separation along the sides of an equilateral triangle is 150 nm, and $\lambda = 473$ nm. From left to right: x, y, z components of the E-field at $\Delta z = 5$ nm below the bottom facet.

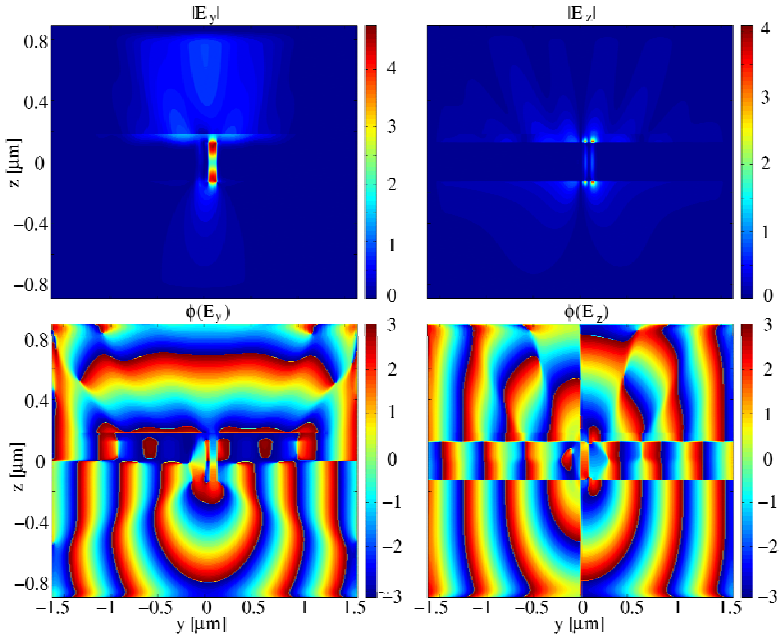

Fig. A2. Amplitude and phase distributions within the cross-sectional yz-plane for transmission through a triplet of 80 nm-diameter holes in a 250 nm-thick silver film. Simulation parameters are the same as those of Fig. A1.

Acknowledgement

This work has been supported by the Air Force Office of Scientific Research under contract number FA 9550–04–1–0213.

#112667 - $15.00 USD Received 11 Jun 2009; revised 14 Jul 2009; accepted 15 Jul 2009; published 28 Jul 2009